ASITP

INSTITUTE OF THEORETICAL PHYSICS ACADEMIA SINICA

AS-ITP-94-46
September 1994

New Approach to determine the Spin of Superdeformed band

J.Y. Zeng Y.A. Lei
and W.Q. Wu

P.O.Box 2735, Beijing 100080, The People's Republic of China

Telefax : (86)-1-2562587 Telephone : 2568348
Telex : 22040 BAOAS CN Cable : 6158

New approach to determine the spin of superdeformed band

J. Y. Zeng[a,b,c], Y. A. Lei[b], and W. Q. Wu[b]

[a]China Center of Advanced Science and Technology (World Laboratory),
Center of Theoretical Physics, P. O. Box 8730, Beijing 100080

[b]Department of Physics, Peking University, Beijing 100871

[c]Institute of Theoretical Physics, Chinese Academy of Sciences, Beijing 100080

Abstract

Based on the very general properties of the rotational band of axially symmetric nuclei demonstrated by Bohr and Mottelson, some rules of the I variation of the kinematic and dynamic moments of inertia are obtained, which may serve as the effective criteria of the spin assignment of rotational band. Using these criteria, the level spins of 37 SD bands in the $A \sim 190$ region are determined unambiguously. Hence, the kinematic moment of inertia $J^{(1)}$ can be extracted directly from the experimental transition energy and compared with the corresponding dynamic moment of inertia $J^{(2)}$. The systematic odd-even differences in $J^{(1)}$ (in the whole spin range observed) and in $J^{(2)}$ (in the low spin range) are established. The comparison of the $J^{(1)}$ and $J^{(2)}$ of identical SD bands is discussed.

PACS numbers: 21.10.re, 21.60 Ev.

I. INTRODUCTION

Since the discovery of the superdeformed (SD) band in ^{191}Hg [1], the region of SD nuclei with mass $A \sim 190$ has been studied extensively over the last few years [2] and a great number of SD bands have been discovered. The experimental data on SD bands consist in a series of γ-ray energies linking levels of unknown spin, so the experimentalists have no choice but to deal with the dynamic moment of inertia $J^{(2)}$, rather than the kinematic moment of inertia $J^{(1)}$. Usually, the kinematic moment of inertia is extracted from the experimental γ-ray energy E_γ using the relation

$$J^{(1)}(I-1)/\hbar^2 = (2I-1)/E_\gamma(I \to I-2), \tag{1}$$

which depends on the level spins, while in the extraction of the dynamic moment of inertia only the differences in E_γ's are involved and there is no need of spin assignment

$$J^{(2)}(I)/\hbar^2 = \frac{4}{\Delta E_\gamma(I)} = \frac{4}{E_\gamma(I+2 \to I) - E_\gamma(I \to I-2)}. \tag{2}$$

This extraction is mode-independent and is generally considered to be reliable provided the moments of inertia vary smoothly with the angular momentum (i.e., the local $I(I+1)$ rule for the rotational spectra holds). It is well known that the relative errors in E_γ's are usually rather small ($\delta E_\gamma < 1$ keV, $\delta E_\gamma/E_\gamma \sim 10^{-3}$), but the relative errors in ΔE_γ's are larger by at least an order of magnitude ($\delta \Delta E_\gamma \sim 1$ keV, $\Delta E_\gamma \sim 50$ keV, $\delta \Delta E_\gamma/\Delta E_\gamma \sim 2 \times 10^{-2}$), so the uncertainty in the extracted $J^{(2)}$ is usually rather large. Obviously, the level spin determination is fundamental to understanding the physics of the new regime of deformation. As yet several approaches to determine the level spins of SD band have been developed [3—6]. All these approaches invoke the least squares fit of the experimental data (on $J^{(2)}$'s

[3,4], or on E_γ's [5,6]) to certain model-dependent expression for rotational spectra. It is interesting to note that the same spin assignments were obtained by these approaches for the SD bands in the $A \sim 190$ region (except for a few cases: ^{189}Hg(1), ^{190}Hg(1) and ^{191}Hg(1)). However, there have been some comments on the uncertainties in these spin assignments [7,8], and some people still take a skeptical attitude.

Careful investigation shows that there exists close connection between the features of both kinds of moments of inertia, which seems not to attract attention. In Sect. II we will show that, based on the very general properties of rotational spectra, demonstrated by Bohr and Mottelson [9], some simple and illustrative criteria of the spin assignment of rotational band can be derived from the investigation of the I variations of $J^{(1)}$ and $J^{(2)}$, and may be used effectively to determine the level spins of SD bands. In Sect. III the 37 SD bands available in the $A \sim 190$ region are addressed and the level spins of these SD bands are determined unambiguously. Once the level spins are determined, the experimental kinematic moment of inertia can be extracted directly from the experimental E_γ's using eq. (1) and compared with the theoretical value calculated using certain model-dependent formulae. From the extracted and calculated $J^{(1)}$ and $J^{(2)}$, several important observations can be made, including the odd-even differences in $J^{(1)}$ and $J^{(2)}$, the similarities and differences between identical SD bands, etc., which are presented in Sect. IV. A brief summary is given in Sect. V.

II. CRITERIA OF THE SPIN ASSIGNMENT OF ROTATIONAL BAND

According to the famous work by Bohr and Mottelson [9], the $K = 0$ rotational spectrum of an axially symmetric nucleus, under the adiabatic approximation, can

be expressed as a function of $I(I+1)$ and expanded in powers of $I(I+1)$. Let $\xi = \sqrt{I(I+1)}$, the rotational energy can be expressed as

$$E = A\xi^2 + B\xi^4 + C\xi^6 + D\xi^8 + \cdots \tag{3}$$

The expression for the rotational energy of $K \neq 0$ band [9] takes a form similar to eq(3), but includes a band-head energy, and $I(I+1)$ is replaced by $I(I+1) - K^2$. It was well established that the extensive experimental data on nuclear rotational bands (below bandcrossing) of normally deformed nuclei are described very well by eq. (3). Systematic analysis of the large amount of data on the rotational spectra of rare-earth and actinide nuclei showed [9,10] that $|B/A| \sim 10^{-3}$, $|C/A| \sim 10^{-6}$, $|D/A| \sim 10^{-9}$, etc.; i.e. the convergence of the $I(I+1)$ expansion (3) is satisfactory, hence the two-parameter AB expression (putting $C = D = \cdots = 0$ in eq. (3)) is widely used for the approximate description of rotational spectra. For the SD bands, the convergence is even better [4] ($|B/A| \sim 10^{-4}$, $|C/A| \sim 10^{-8}$, etc.), i.e., compared to the normally deformed nuclei, the SD nucleus appears to be a more rigid rotator with axial symmetry. From eq.(3) the kinematic and dynamic moments of inertia [11],

$$J^{(1)}/\hbar^2 = \xi \Big/ \frac{dE}{d\xi}, \quad J^{(2)}/\hbar^2 = \left(\frac{d^2E}{d\xi^2}\right)^{-1}, \tag{4}$$

are expressed as

$$J^{(1)}/\hbar^2 = \frac{1}{2A}(1 + 2\frac{B}{A}\xi^2 + 3\frac{C}{A}\xi^4 + \cdots)^{-1}, \tag{5}$$

$$J^{(2)}/\hbar^2 = \frac{1}{2A}(1 + 6\frac{B}{A}\xi^2 + 15\frac{C}{A}\xi^4 + \cdots)^{-1}. \tag{6}$$

Hence, we have

$$\lim_{I\to 0} J^{(1)}/\hbar^2 = \lim_{I\to 0} J^{(2)}/\hbar^2 = 1/2A, \tag{7}$$

$$\sqrt{J^{(1)3}/J^{(2)}} = \frac{\hbar^2}{2A}\left\{1 - 3\left[6\left(\frac{B}{A}\right)^2 - \frac{C}{A}\right]\xi^4 + \cdots\right\} \approx \frac{\hbar^2}{2A}. \tag{8}$$

It is also easily verified that

$$\frac{1}{\hbar^2}\frac{dJ^{(1)}}{d\xi} = -2\frac{B}{A^2}\xi\left[1 - \left(\frac{4B}{A} - \frac{3C}{B}\right)\xi^2 + \cdots\right], \tag{9}$$

$$\frac{1}{\hbar^2}\frac{dJ^{(2)}}{d\xi^2} = -\frac{6B}{A^2}\xi\left[1 - \left(\frac{12B}{A} - \frac{5C}{B}\right)\xi^2 + \cdots\right], \tag{10}$$

$$\lim_{I\to 0}\frac{dJ^{(1)}}{d\xi} = \lim_{I\to 0}\frac{dJ^{(2)}}{d\xi} = 0, \tag{11}$$

$$\frac{dJ^{(2)}}{d\xi}\Big/\frac{dJ^{(1)}}{d\xi} = 3\left[1 - 2(4\frac{B}{A} - \frac{C}{B})\xi^2 + \cdots\right], \tag{12}$$

$$\frac{1}{\hbar^2}\frac{d^2J^{(1)}}{d\xi^2} = -\frac{2B}{A^2}\left[1 - 3\left(\frac{4B}{A} - \frac{3C}{B}\right)\xi^2 + \cdots\right], \tag{13}$$

$$\frac{1}{\hbar^2}\frac{d^2J^{(2)}}{d\xi^2} = -6\frac{B}{A^2}\left[1 - 3\left(\frac{12B}{A} - \frac{5C}{B}\right)\xi^2 + \cdots\right], \tag{14}$$

$$\frac{d^2J^{(1)}}{d\xi^2} = \frac{d^2J^{(2)}}{d\xi^2} = 0 \quad \text{(for a rigid rotator)}, \tag{15}$$

$$\frac{d^2J^{(2)}}{d\xi^2}\Big/\frac{d^2J^{(1)}}{d\xi^2} = 3\left[1 - 6\left(\frac{4B}{A} - \frac{C}{B}\right)\xi^2 + \cdots\right]. \tag{16}$$

From eqs. (5)—(16), several rules can be observed:

(a) As $I \to 0$, both $J^{(1)}$ and $J^{(2)}$ of the same band tend to the same limiting value (bandhead moment of inertia).

(b) Both $J^{(1)}$ and $J^{(2)}$ *monotonously increase with* I (for $B < 0$), or *monotonously decrease with* I (for $B > 0$), but the slope of $J^{(2)}$ is much steeper than that of $J^{(1)}$ ($dJ^{(2)}/d\xi \approx 3dJ^{(1)}/d\xi$ in the low spin range).

(c) Hence, $J^{(1)}$-ξ and $J^{(2)}$-ξ plots *never cross each other* at any nonzero spin value.

(d) As $I \to 0$, both the slopes of $J^{(1)}$ and $J^{(2)}$ tend to zero , i.e., both $J^{(1)}$-ξ and $J^{(2)}$-ξ plots become horizontal.

(e) *Both* $J^{(1)}$-ξ and $J^{(2)}$-ξ plots *concave upwards* (for $B < 0$), or *concave downwards* (for $B > 0$).

(f) $\sqrt{J^{(1)3}/J^{(2)}}$ = constant (bandhead moment of inertia) holds for not too high spin.

Extensive analysis of large amount of available rotational bands (below band-crossing) of normally deformed nuclei whose spins are established shows that these six rules do hold without exception. In Fig. 1 we give an illustrative example, the analysis of the ground rotational band of the well-deformed nucleus, ^{242}Pu. In Fig. 1(c), are displayed the $J^{(1)}$ and $J^{(2)}$ extracted by eqs. (1) and (2) from the experimental rotational spectrum using the established spin sequence I = 0, 2, 4, $\cdots$. Fig. 1(c) is a standard pattern of $J^{(1)}$-ξ and $J^{(2)}$-ξ plots of well-deformed nuclei whose spins are measured, and the $J^{(1)}$-ξ and $J^{(2)}$-ξ plots for other rotational bands are quite similar. However, if one artificially changes the spin sequence, some of these rules may obviously fail. For example, if the spin of each level is artificially increased by 1 $\hbar$ (Fig. 1(d)) or 2 $\hbar$ (Fig. 1(e)), i.e., the measured spin sequence 0, 2, 4, $\cdots$ is replaced by 1, 3, 5, $\cdots$ or 2, 4, 6, $\cdots$, the pattern of $J^{(1)}$-ξ will change. Particularly, in the low spin range, the extracted $J^{(1)}$ increases significantly (the lower the level spin, the larger the increase of $J^{(1)}$ value), and the $J^{(1)}$-ξ plot concaves upwards. However, it is seen from eq. (2) that the *pattern* of the extracted $J^{(2)}$ is not influenced by the change of spin sequence, and for different assignments of the spin sequence the $J^{(2)}$-ξ plot is only displaced as a whole. From Figs. 1(d)

and (e), it is seen that: (i) $J^{(1)}$-ξ and $J^{(2)}$-ξ plots cross each other at certain spin I_c. (ii) For $I > I_c$, $J^{(1)}$ decreases with decreasing I, but as $I \to 0$, $J^{(1)}$ increases with decreasing I, i.e., its monotonousness is broken. (iii) As $I \to 0$, $J^{(1)}$-ξ plot does not become horizontal, and $J^{(1)}$ does not tend to the same limiting value as that of $J^{(2)}$. On the other hand, if the spin of each level is artificially decreased by 1 $\hbar$ (Fig. 1(b)) or 2 $\hbar$ (Fig. 1(a)), i.e., the measured spin sequence 0, 2, 4, 6, $\cdots$ is replaced by -1 (unphysical), 1, 3, 5, $\cdots$, or -2 (unphysical), 0, 2, 4, $\cdots$, the extracted $J^{(1)}$ decreases to various extents (the lower the level spin, the larger the decrease of $J^{(1)}$ value). It is seen from Figs. 1(b) and (a) that: (i) In the low spin range, the slope of $J^{(1)}$ increase with decreasing I and does not tend to zero as $I \to 0$. (ii) As $I \to 0$, $J^{(1)}$ does not tend to the same limiting value as $J^{(2)}$. (iii) In the low spin range, $J^{(1)}$-ξ plot becomes concave downwards.

Therefore, for a rotational band whose level spins are unknown, we may assume a spin sequence, I_0, I_0+2, I_0+4, $\cdots$, and then construct the $J^{(1)}$-ξ and $J^{(2)}$-ξ plots using eqs. (1) and (2) from the measured intraband γ ray energies. In this case, violation of one (or more) of the six rules implies an unreasonable spin assignment is made, hence such spin assignment must be ruled out. Analysis shows that using this procedure we can find out the reasonable spin assignment of a rotational band whose spins are unknown. The advantage of this approach over the previous ones [3—6] is that it does not involve the least squares fit of the experimental data to some model-dependent formulae for rotational spectra.

Now we use the rules mentioned above as the criteria of the spin assignment of SD bands. Fig. 2 give an illustrative example, the SD band ^{194}Hg(1), $E_\gamma(I_0+2 \to I_0) = 254.3$ keV. (The systematic analysis of the SD bands available in the $A \sim 190$ region is given in Sect. III.) In Fig. 2, several spin assignments $I_0 = 8$, 9, 10, 11,

and 12 are assumed. It is seen that, on one hand, the spin assignments $I_0 \geq 11$ are obviously forbidden by the rules (c), (a), (b) and (d). On the other hand, the spin assignments $I_0 \leq 9$ are ruled out by the rules (e), (d) and (a). Therefore, only the spin assignment $I_0 = 10$ (Fig. 2(c)) is allowed, which is the same as that given in refs. [4,5,6].

It should be noted that the six rules drawn above remain valid in the Harris ω expansion [9,12]

$$E = \alpha\omega^2 + \beta\omega^4 + \gamma\omega^6 + \delta\omega^8 + \cdots, \tag{17}$$

of which the convergence is believed [9] to be superior to that of the $I(I+1)$ expansion (3). The rotational frequency ω is defined as

$$\omega = \frac{dE}{d\xi} = 2A\xi + 4B\xi^3 + 6C\xi^5 + 8D\xi^7 + \cdots, \tag{18}$$

so

$$\xi = \int \frac{dE}{\omega} = 2\alpha\omega + \frac{4}{3}\beta\omega^3 + \frac{6}{5}\gamma\omega^5 + \frac{8}{7}\delta\omega^7 + \cdots. \tag{19}$$

Hence, it is easily verified that

$$J^{(1)}/\hbar^2 = 2\alpha + \frac{4}{3}\beta\omega^2 + \frac{6}{5}\gamma\omega^4 + \cdots, \tag{20}$$

$$J^{(2)}/\hbar^2 = 2\alpha + 4\beta\omega^2 + 6\gamma\omega^4 + \cdots, \tag{21}$$

$$\lim_{\omega\to 0} J^{(1)}/\hbar^2 = \lim_{\omega\to 0} J^{(2)}/\hbar^2 = 2\alpha, \tag{22}$$

$$\sqrt{J^{(1)3}/J^{(2)}} = 2\alpha\hbar^2\left\{1 - \left[2\left(\frac{\beta}{\alpha}\right)^2 - \frac{3}{5}\frac{\gamma}{\alpha}\right]\omega^4 + \cdots\right\} \approx 2\alpha\hbar^2, \tag{23}$$

$$\frac{1}{\hbar^2}\frac{d}{d\omega}J^{(1)} = \frac{8}{3}\beta\omega + \frac{24}{5}\gamma\omega^3 + \cdots, \tag{24}$$

$$\frac{1}{\hbar^2}\frac{d}{d\omega}J^{(2)} = 8\beta\omega + 24\gamma\omega^3 + \cdots, \tag{25}$$

$$\lim_{\omega\to 0}\frac{dJ^{(1)}}{d\omega} = \lim_{\omega\to 0}\frac{dJ^{(2)}}{d\omega} = 0, \tag{26}$$

$$\frac{dJ^{(2)}}{d\omega}\Big/\frac{dJ^{(1)}}{d\omega} = 3\left(1 + \frac{6}{5}\frac{\gamma}{\beta}\omega^2 + \cdots\right). \tag{27}$$

Particularly, for the widely used Harris 2 parameter expansion (putting $\gamma = \delta = \cdots = 0$ in eq.(17))

$$\frac{dJ^{(2)}}{d\omega}\Big/\frac{dJ^{(1)}}{d\omega} = 3, \tag{28}$$

$$\frac{d^2J^{(1)}}{d\xi^2} = \frac{1}{3}\frac{d^2J^{(2)}}{d\xi} = \frac{8}{3}\beta\hbar^2. \tag{29}$$

Similarly, the same rules can also be drawn from the less known abc expression for rotational spectra [13]

$$E = a[\sqrt{1+b\xi^2} - 1] + c\xi^2, \tag{30}$$

which can be derived from the Bohr Hamiltonian (including an anharmonic potential term $k\beta^4$) of well-deformed nuclei with small axial asymmetry ($\sin^2 3\gamma \ll 1$). c may be positive or negative according to the sign of k and $|c/a| \ll 1$ (see Table II). For $c = 0$, eq. (30) is reduced to the ab expression

$$E = a[\sqrt{1+b\xi^2} - 1], \tag{31}$$

which was suggested empirically many years ago by Hohmberg and Lipas [14] and was rederived from the Bohr Hamiltonian [15,16]. From eqs. (30) and (4) we have

$$J^{(1)}/\hbar^2 = \left[ab(1+b\xi^2)^{-1/2} + 2c\right]^{-1}, \tag{32}$$

$$J^{(2)}/\hbar^2 = \left[ab(1+b\xi^2)^{-3/2} + 2c\right]^{-1}, \tag{33}$$

$$\lim_{I\to 0} J^{(1)}/\hbar^2 = \lim_{I\to 0} J^{(2)}/\hbar^2 = 1/ab. \tag{34}$$

For the simplified ab expression (31), the expressions of $J^{(1)}$ and $J^{(2)}$ become very simple and

$$\sqrt{J^{(1)3}/J^{(2)}} = J_0, \quad (J_0 = \hbar^2/ab), \tag{35}$$

is I-independent, (J_0 is the bandhead moment of inertia), which has been shown to hold excellently for normally deformed nuclei [17].

III. SPIN ASSIGNMENT OF THE SD BANDS IN THE $A \sim 190$ REGION

Using the procedure to determine the spin sequence of a rotational band outlined in Sect. II, the level spins of 37 SD bands available in the $A \sim 190$ region have been determined unambiguously and the results are summarized in Table I. For the detailed analysis of each SD band, see Figs. (3)—(9).

It is interesting to note that the spin assignments obtained by the present approach are the same as those given in refs. [3—6] except of a few cases (^{189}Hg(1), ^{191}Hg(1), and ^{190}Hg(1)). To confirm the reliability of the present spin assignments for these three SD bands, we may use the additional rule (f); i.e., $\sqrt{J^{(1)3}/J^{(2)}}$ should be I-independent for not too high spin (see eq. (8)). The results are displayed in Fig. 10. It is seen that for the SD bands ^{189}Hg(1) and ^{191}Hg(1), $I_0 \leq 14.5$ and $I_0 \geq 16.5$ are forbidden by the rule (f), and $I_0 = 15.5$ is the unique plausible candidate. Similarly, for the yrast SD band ^{190}Hg(1), $E_\gamma = 360$ keV, $I_0 = 14$ is the most plausible candidate.

It is noted: (i) All the yrast SD bands in even-even nuclei have signature ($\alpha = 0$) (I even). (ii) For the 37 SD bands now available in the $A \sim 190$ region, the spin of the lowest level observed is not too high ($I_0 \sim (6\text{–}37/2) < 20$), which may be the reason that the spin assignment can be made unambiguously.

IV. MOMENTS OF INERTIA AND DISCUSSIONS

Once the level spins of a rotational band are determined, using eq. (1) one may extract the experimental kinematic moments of inertia directly from the γ-ray energies observed. From the extracted $J^{(1)}$ and $J^{(2)}$ of the SD bands in the $A \sim 190$ region, systematic odd-even differences in the moments of inertia can be established, which is discussed in Sect. IV.A. On the other hand, the observed transition energies can be least squares fit to a suitable analytic expression for rotational spectra, and then the moments of inertia can be calculated by the corresponding analytic expressions and compared with the experimental ones, which are presented in Sect. IV.B. In Sect. IV.C the comparison of the moments of inertia of identical SD bands is addressed. Similarities and differences between the SD bands of neighboring even-even nuclei will be discussed in IV.D.

A. Odd-even differences in the moments of inertia of SD bands

From Figs. (3)—(9) it is seen: (i) For all the SD bands in the $A \sim 190$ region (except the excited SD band ^{193}Hg(4) above bandcrossing) $J^{(1)}$ and $J^{(2)}$ increase smoothly with spin in the spin range $I \leq 40\hbar$. (ii) $\frac{dJ^{(2)}}{d\xi} = 3\frac{dJ^{(1)}}{d\xi}$ holds well. (iii) The slope of $J^{(1)}$ ($J^{(2)}$) for the yrast SD bands is steeper in even-even nuclei than in odd-A nuclei, and there is indication that systematic odd-even differences in $J^{(1)}$ and $J^{(2)}$ do exist. To show this, the extracted $J^{(1)}$ and $J^{(2)}$ for $I \sim 10$, 20 and 30

are presented in Fig. 11. It is noted that in the spin range observed ($I \leq 40\hbar$), $J^{(1)}$ (odd-A) $>$ $J^{(1)}$ (yrast SD band in even-even nuclei), and the difference is especially significant at low spins, quite like that observed in normally deformed nuclei [41]. This may be an indication of the influence of pairing interaction and blocking effect in SD nuclei. In contrast, while in the low spin range ($I < 20$) there exists systematic odd-even difference in $J^{(2)}$, with increasing I this odd-even difference gradually disappears.

B. Calculation of moment of inertia

Considering the much larger relative error in ΔE_γ than that in E_γ, it is better to carry out the least squares fit of the experimental E_γ (rather than ΔE_γ or $J^{(2)}$) to a suitable analytic expression (with some parameters) for rotational spectra, and then the moments of inertia can be calculated by the corresponding analytic expressions. In ref. [13] it was shown that all the experimental ground band rotational spectra of well-deformed rare-earth and actinide nuclei can be reproduced excellently by the *abc* expression (30) up to very high spin (below bandcrossing). Considering the features of SD bands (very large quadrupole deformation β, small axial asymmetry $\sin^2 3\gamma \ll 1$, super-rigidity, etc.), which are consistent with the basic assumptions made in the derivation of *abc* expression (30) from the Bohr Hamiltonian [13], we prefer to use the *abc* expression to fit the experimental E_γ's and then calculate $J^{(1)}$ and $J^{(2)}$ using the analytic eqs. (32) and (33). Four examples, the SD bands ^{192}Hg(1), ^{194}Hg(1), ^{194}Hg(2) and ^{194}Hg(3)) are given in Table II. It is encouraging that all the experimental E_γ's, and $J^{(1)}$ and $J^{(2)}$ extracted by eqs. (1) and (2), can be reproduced excellently within the experimental errors. For example, for the SD band ^{194}Hg(2), $|E_{\gamma,\mathrm{calc}} - E_{\gamma,\mathrm{expt}}| \leq 0.3$ keV, $|J^{(1)}_{\mathrm{calc}} - J^{(1)}_{\mathrm{expt}}|/J^{(1)}_{\mathrm{expt}} \leq 10^{-3}$,

$|J^{(2)}_{calc} - J^{(2)}_{expt}|/J^{(2)}_{expt} < 2 \times 10^{-2}$. For the other SD bands in the $A \sim 190$ region, the situation is similar.

In Fig. 12 the comparison of the calculated and experimental $J^{(1)}$ and $J^{(2)}$ for the SD bands ^{192}Hg(1), ^{194}Hg(1), and the signature partners ^{194}Hg(2) and ^{194}Hg(3) are presented. It is seen that the calculated $J^{(1)}$'s (dotted line in Fig. 12) are practically identical to the experimental ones. On the other hand, while the experimental I variation in $J^{(2)}$ is reproduced very well by the calculation (dotted line in Fig. 12), some fluctuations in $J^{(2)}_{expt}$ appear due to the large experimental error in ΔE_γ.

C. Moments of inertia of identical SD bands

Based on the analysis of the dynamic moments of inertia and rotational alignments, the signature partners ^{194}Hg(2) and ^{194}Hg(3) were considered as identical to the SD band ^{192}Hg(1) [33]. In Fig. 13 the comparison of the $J^{(1)}$ and $J^{(2)}$ for the SD bands ^{194}Hg(2,3) and ^{192}Hg(1) are displayed. From Fig. 13 several observations can be made: (a) In the spin range $I \sim 20$—40 ($\hbar\omega \sim 0.2$—0.4 MeV) the $J^{(2)}$ values of the SD bands ^{194}Hg(2,3) do nearly equal to the corresponding $J^{(2)}$ values of ^{192}Hg(1). (b) However, at the low spin range $I < 20$ ($\hbar\omega < 0.2$ MeV), the $J^{(2)}$ values of ^{194}Hg(2,3) are systematically larger than the corresponding $J^{(2)}$ values of ^{192}Hg(1). (c) The $J^{(1)}$ values of ^{194}Hg(2,3) are systematically larger than those of ^{192}Hg(1). Similar situation occurs for the two pairs of signature partner SD bands ^{191}Hg(2,3) and ^{193}Hg(2b,3), which are displayed in Figs. 14 and 15.

It has been noted [42,43] that the identical bands are also present in normally deformed pairs of even- and odd-mass nuclei. An example is displayed in Figs. 16. It is seen that at high spins $I \geq 10$, the $J^{(2)}$ values of the $[633]5/2^+$ band are nearly equal to the corresponding $J^{(2)}$ values of the ground band of ^{236}U.

D. Similarities between SD bands in neighboring even-even nuclei

Though the yrast SD bands of ^{192}Hg(1) and ^{194}Hg(1) are usually not considered as identical, they are in fact quite similar to each other in the whole spin range observed $I \leq 40$ (Fig. 17). Similar situations occur for the yrast SD bands in ^{194}Pb and ^{192}Hg(1) (Fig. 18), and ^{196}Pb and ^{198}Pb (Fig. 19). Similarities between the ground bands of neighboring normally deformed even-even nuclei [44,45] have been recognized for a long time, which may be considered as an indication of strong pairing correlation and nuclear superconductivity. In fact, the extracted $J^{(1)}$ and $J^{(2)}$ values of the ground bands of ^{236}U and ^{238}U are almost identical to each other in the whole spin range $I < 26$ (below bandcrossing).

V. SUMMARY

In summary, based on the investigation of the general properties of rotational spectra of axially symmetric nuclei, some simple and illustrative rules for the I variations of $J^{(1)}$ and $J^{(2)}$ are derived, which may be used as effective criteria to determine the spin sequence of a rotational band. The advantage of this new approach over the previous ones is that it does not involve the least squares fit of experimental data (on $J^{(2)}$ or E_γ) to some model-dependent expression for rotational spectra. The 37 SD bands in the $A \sim 190$ region have been determined unambiguously. Using the spins thus determined, some important features of the $J^{(1)}$ and $J^{(2)}$ moments of inertia of these SD bands are investigated, including the systematic odd-even differences in $J^{(1)}$ (in the whole observed spin range) and in $J^{(2)}$ (in the low spin range), the similarities and differences in $J^{(1)}$ and $J^{(2)}$ of identical SD bands, etc., which are very useful for understanding the intrinsic configurations of these SD bands.

References

[1] E. F. Moore et al., Phys. Rev. Lett. **63**, 360(1989).

[2] See the review papers, e.g., R. V. F. Janssens and T. L. Khoo, Annu. Rev. Part. Nucl. Sci. **41**, 321 (1991); P. J. Twin, Nucl. Phys. **A520**, 17c(1990).

[3] J. E. Draper et al., Phys. Rev. C **42**, R1791 (1991).

[4] J. A. Becker et al., Phys. Rev. C **46**, 889(1992); Nucl. Phys. A **520**, 187c(1990).

[5] J. Y. Zeng, J. Meng, C. S. Wu, E. G. Zhao, Z. Xing and X. Q. Chen, Phy. Rev. C **44**, R1745(1991). C. S. Wu, J. Y. Zeng, Z. Xing, X. Q. Chen and J. Meng, Phys. Rev. C **45**, 261(1992).

[6] R. Piepenbring and K. V. Protasov, Z. Phys. **A 345**, 7(1993).

[7] C. L. Wu, D. H. Feng and A. W. Guidry, Phys. Rev. lett. **66**, 1377(1991).

[8] R. A. Wyss and S. Pilotte, Phys. Rev. C**44**, R602 (1991).

[9] A. Bohr and B. R. Mottelson, *Nuclear Structure*, Vol. 2, (1975, Benjamin).

[10] F. X. Xu, C. S. Wu and J. Y. Zeng, Phys. Rev. C**40**, 2337(1989).

[11] I. Hamamoto, Treatise on Heavy-Ion Science, **3**, 313(1985, Plenum).

[12] S. M. Harris, Phys. Rev. **138**, B 509(1965).

[13] H. X. Huang, C. S. Wu and J. Y. Zeng, Phys. Rev. C**39**, 1617 (1989).

[14] P. Holmberg and P. C. Lipas, Nucl. Phys. **A117**, 552(1967).

[15] C. S. Wu and J. Y. Zeng, Commu. Theor. Phys. **8**, 51(1987).

[16] C. S. Wu and J. Y. Zeng, High Energy Phys. Nucl. Phys. 8, 219, 445(1984), 9, 77, 214(1985), (in Chinese).

[17] C. S. Wu, Li Cheng, C. Z. Lin and J. Y. Zeng, Phys. Rev. C**45**, 2507 (1992).

[18] D. T. Vo et al., Phys. Rev. Lett. **71**, 340(1993).

[19] S. Pilotte et al., Phys. Rev. C**49**, 718(1994).

[20] B. F. Fernandez et al., Nucl. Phys. **A517**, 386(1990).

[21] R. V. F. Janssens et al., Nucl. Phys. **A520**, 75c(1990).

[22] F. Azaiez et al., Z. Phys. **A338**, 471(1991).

[23] J. Duprat et al., private communication.

[24] H. W. Carpenter et al., Nucl. Phys. **A530**, 452(1991).

[25] M. P. Carpenter et al., PL(B240), 44(1990).

[26] D. M. Cullen et al., Phys. Rev. **A520**, 105c(1990).

[27] M. J. Joyce et al., Phys. Rev. Lett. **71**, 2176(1993).

[28] J. A. Becker et al., Phys. Rev. C**41**, R9(1990).

[29] D. Ye et al., Phys. Rev. C**41**, R13(1990).

[30] E. F. Moore et al., Phys. Rev. Lett. **23**, 3127(1990).

[31] T. Lauritsen et al., PL(B279), 237(1992).

[32] C. W. Beausang et al., Z. Phys. **A335**, 325(1990).

[33] F. S. Stephens et al., Phys. Rev. Lett. **64**, 2623(1990).

[34] E. A. Henry et al., Z. Phys. **A339**, 469(1991).

[35] J. Brinkman et al., Z. Phys. **A336**, 115(1990).

[36] W. Korten et al., Z. Phys. **A344**, 475(1993).

[37] E. F. Moore et al., Phys. Rev. C**48**, 2261(1993).

[38] T. F. Wang et al., Phys. Rev. C43, R2645(1991).

[39] F. Azaiez et al., Phys. Rev. Lett. 66, 1030(1991).

[40] Y. Liang et al., Phys. Rev. C46, R2136(1992).

[41] J. Y. Zeng, Y. A. Lei, T. H. Jin and Z. J. Zhao, Phys. Rev. C50, No. 2, Aug., (1994).

[42] C. Baktash, J. D. Garrett, D. F. Winchell, and A. Smith, Phys. Rev. Lett. 69, 1500(1992).

[43] Jing-ye Zhang and L. L. Riedinger, Phys. Rev. Lett. 69, 3448(1992).

[44] I. Ahmad, M. P. Carpenter, R. R. Chasman, R. V. F. Janssens and T. L. Khoo, Phys. Rev. C44, 1204(1991).

[45] R. F. Casten, V. V. Zamfir, D. Von Brentano, and W. T. Chou, Phys. Rev. C45, 1413(1992).

Table Captions

Table I Spin assignment of the SD bands in the $A \sim 190$ region. (a) Odd-A nuclei. (b) Even-even nuclei. (c) Odd-odd nuclei.

Table II Comparison of the experimental and calculated transition energy E_γ (in units keV). $J^{(1)}$ and $J^{(2)}$ (in units $\hbar^2\mathrm{MeV}^{-1}$) of the SD bands: (a) ^{192}Hg(1), (b) ^{194}Hg(1), (c) ^{194}Hg(2) and (d) ^{194}Hg(3).

Table I

(a) Odd-A nuclei

	$E_\gamma(I_0+2\rightarrow I_0)$	I_0			
SD band	keV	a	b	c	present
^{191}Au	229.5[d]				19/2
^{191}Tl(1)	358.9[e]				31/2
^{191}Tl(2)	417.2[e]				37/2
^{193}Tl(1)	228.1[f]	19/2	19/2	19/2	19/2
^{193}Tl(2)	248.3[f]	21/2	21/2	21/2	21/2
^{195}Tl(1)	146.2[g]				11/2
	350.7[g]	(31/2)			31/2
^{195}Tl(2)	208.4[g]				17/2
	330.1[g]	(29/2)			29/2
^{189}Hg(1)	366.0[h]	(29/2*,31/2)		29/2	31/2
^{191}Hg(1)	350.6[i]	(29/2*,31/2)	31/2	29/2	31/2
^{191}Hg(2)	292.0[j]	25/2	25/2	25/2	25/2
^{191}Hg(3)	311.8[j]	27/2	27/2	27/2	27/2
^{193}Hg(3)	233.7[k]		19/2	19/2	19/2
^{193}Hg(2b)	254.3[k]	21/2	21/2	21/2	21/2
^{193}Hg(1)	192.6[k]	15/2	15/2		15/2
^{193}Hg(2a)	254.3[k]		21/2	21/2	21/2
^{193}Hg(4)	290.5[k]		27/2		29/2

[a]Ref. [4], [b]Ref. [5], [c]Ref. [6], [d]Ref. [18], [e]Ref. [19], [f]Ref. [20,21], [g]Ref. [22,23], [h]Ref. [24], [i]Ref. [1], [j]Ref. [25], [k]Ref. [26,27].

Table I (continued)

(b) Even-even nuclei

	$E_\gamma(I_0+2\rightarrow I_0)$	I_0			
SD band	keV	a	b	c	present
^{190}Hg(1)	360.0[d]	14	15	14	14
^{192}Hg(1)	214.6[e]	8	8	8	8
^{194}Hg(1)	254.3[f]	10	10	10	10
^{194}Hg(2)	201.3[g]	8	8	8	8
^{194}Hg(3)	262.3[g]	11	11	11	11
^{192}Pb	262.6[h]	10*, 11			10
^{194}Pb	169.6[i]	6	6	6	6
^{196}Pb	169.9[j]				6
	214.8[j]	8	8	8	8
^{198}Pb	303.8[k]	12			12

[a]Ref. [4], [b]Ref. [5], [c]Ref. [6], [d]Ref. [21], [e]Ref. [28—31], [f]Ref. [32], [g]Ref. [33], [h]Ref. [34], [i]Ref. [35,36], [j]Ref. [37,38], [k]Ref. [38].

Table I (continued)

(c) Odd-odd nuclei

	$E_\gamma(I_0+2\rightarrow I_0)$	I_0			
SD band	keV	a	b	c	present
^{194}Tl(1a)	268.0[d]	12	12	12	12
^{194}Tl(1b)	209.3[d]	9	9	9	9
^{194}Tl(2a)	280.0[d]				12
	240.5[d]	(10$^+$,11)	10	10	10
^{194}Tl(2b)	259.4[d]				11
	220.5[d]	(9$^+$,10)	9	9	9
^{194}Tl(3a)	187.9[d]		8	8	8
	226.3[d]	(10$^+$,11)			10
^{194}Tl(3b)	207.0[d]		9	9	9
	245.4[d]	(11$^+$,12)			11
^{192}Tl(1)	357.8[e]				16
^{192}Tl(2)	378.0[e]				17
^{192}Tl(3)	375.7[e]				18
^{192}Tl(4)	357.0[e]				17
^{192}Tl(5)	381.2[e]				16
^{192}Tl(6)	406.5[e]				17

[a]Ref. [4], [b]Ref. [5], [c]Ref. [6], [d]Ref. [39], [e]Ref. [40].

Table II

	(a) ^{192}Hg(1)						(b) ^{194}Hg(1)					
I	$E_\gamma(I\rightarrow I-2)$		$J^{(1)}(I-1)$		$J^{(2)}(I)$		$E_\gamma(I\rightarrow I-2)$		$J^{(1)}(I-1)$		$J^{(2)}(I)$	
	expt.	calc.[a]	expt.	calc.[a]	expt.	calc.[a]	expt.	calc.[b]	expt.	calc.[b]	expt.	calc.[b]
46							841.0	840.7	108.2	108.2		
44							812.9	812.7	107.0	107.0	142.3	142.9
42	793.4	793.4	104.6	104.6			783.9	784.1	105.9	105.8	137.9	140.0
40	762.8	763.0	103.6	103.5	130.7	131.7	754.6	754.9	104.7	104.6	136.5	136.9
38	732.1	732.1	102.4	102.4	130.3	129.4	725.4	725.0	103.4	103.4	137.0	133.7
36	700.6	700.6	101.3	101.3	127.0	127.0	693.8	694.3	102.3	102.3	126.6	130.5
34	668.6	668.5	100.2	100.2	125.0	124.5	662.4	662.9	101.1	101.1	127.4	127.2
32	635.8	635.7	99.1	99.1	122.0	121.9	630.5	630.6	99.9	99.9	125.4	123.9
30	602.3	602.1	98.0	98.0	119.4	119.1	597.3	597.4	98.8	98.8	120.5	120.6
28	567.9	567.7	96.8	96.9	116.3	116.3	563.6	563.3	97.6	97.6	118.7	117.3
26	532.4	532.4	95.8	95.8	112.7	113.4	528.3	528.2	96.5	96.5	113.3	114.1
24	496.3	496.3	94.7	94.7	110.8	110.5	492.3	492.2	95.5	95.5	111.1	110.9
22	459.1	459.1	93.7	93.7	107.5	107.6	455.2	455.1	94.5	94.5	107.8	107.8
20	420.8	420.9	92.7	92.7	104.4	104.7	417.1	416.9	93.5	93.5	105.0	104.9
18	381.6	381.7	91.7	91.7	102.0	101.9	377.8	377.8	92.6	92.6	101.8	102.1
16	341.1	341.4	90.9	90.8	98.8	99.3	337.7	337.6	91.8	91.8	99.8	99.5
14	299.9	300.0	90.0	90.0	97.1	96.8	296.2	296.4	91.2	91.1	96.4	97.2
12	257.7	257.7	89.3	89.2	94.8	94.5	254.3	254.3	90.4	90.4	95.5	95.0
10	214.6	214.4	88.5	88.6	92.8	92.4						

[a] $a = 6597$ keV, $b = 8.168 \times 10^{-4}$, $c = 3.0428$ keV.

[b] $a = 10860$ keV, $b = 5.796 \times 10^{-4}$, $c = 2.4983$ keV.

Table II (continued)

	(c) ^{194}Hg(2)						(d) ^{194}Hg(3)					
I	$E_\gamma(I\rightarrow I-2)$		$J^{(1)}(I-1)$		$J^{(2)}(I)$		$E_\gamma(I-1\rightarrow I-3)$		$J^{(1)}(I-2)$		$J^{(2)}(I-1)$	
	expt.	calc.[c]	expt.	calc.[c]	expt.	calc.[c]	expt.	calc.[d]	expt.	calc.[d]	expt.	calc.[d]
44	807.0	807.0	107.8	107.8	98.5	139.2	793.0	793.0	107.2	107.2		
42	777.7	777.6	106.7	106.7	136.5	135.9	762.7	762.8	106.2	106.2	132.0	132.7
40	747.6	747.5	105.7	105.7	132.9	132.7	732.2	732.0	105.2	105.2	131.1	129.7
38	716.7	716.6	104.6	104.7	129.4	129.5	700.4	700.4	104.2	104.2	125.8	126.8
36	684.5	684.9	103.7	103.7	124.2	126.3	668.0	668.1	103.3	103.3	123.5	123.9
34	652.2	652.4	102.7	102.7	123.8	123.2	635.1	635.0	102.3	102.3	121.6	121.0
32	619.3	619.2	101.7	101.7	121.6	120.2	600.9	601.2	101.5	101.5	117.0	118.3
30	585.2	585.1	100.8	100.8	117.3	117.3	566.4	566.6	100.6	100.6	115.9	115.6
28	550.3	550.1	99.9	100.0	114.6	114.5	531.6	531.2	99.7	99.8	114.9	113.0
26	514.3	514.4	99.2	99.1	111.1	111.9	494.6	495.0	99.1	99.0	108.1	110.5
24	477.7	477.8	98.4	98.4	109.3	109.4	458.3	458.1	98.2	98.2	110.2	108.2
22	440.7	440.5	97.6	97.6	108.1	107.0	420.4	420.3	97.5	97.5	105.5	106.0
20	402.1	402.3	97.0	96.9	103.6	104.8	382.1	381.8	96.8	96.9	104.4	103.9
18	363.7	363.4	96.2	96.3	104.2	102.8	342.8	342.6	96.3	96.3	101.8	102.1
16	323.8	323.8	95.7	95.7	100.3	101.0	302.5	302.8	95.9	95.8	99.3	100.3
14	283.3	283.5	95.3	95.2	98.8	99.3	262.3	262.3	95.3	95.3	99.5	98.8
12	242.7	242.7	94.8	94.8	98.5	97.9						
10	201.3	201.3	94.4	94.4	96.6	96.6						

[c] $a = 22050$ keV, $b = 3.103 \times 10^{-4}$, $c = 1.9229$ keV.

[d] $a = 19240$ keV, $b = 3.297 \times 10^{-4}$, $c = 2.1532$ keV.

Figure Captions

Fig. 1 $J^{(1)}$ and $J^{(2)}$ of the ground rotational band of the normally deformed nucleus ^{242}Pu. $J^{(1)}$ and $J^{(2)}$ are extracted directly from the experimental γ-ray energy using eqs. (1) and (2). In Fig. 1(c), the observed spin sequence $I = 0, 2, 4, 6, \cdots$ is used. In Figs 1(d) and (e), the spin of each level is artificially increased by 1 and 2, i.e., the spin sequence 0, 2, 4, 6, $\cdots$ is replaced by 1, 3, 5, 7, $\cdots$, and 2, 4, 6, 8, $\cdots$. Similarly, the spin sequence adopted in Fig. 1(b) is -1 (unphysical), 1, 3, 5, $\cdots$, and in Fig. 1(a), is: -2 (unphysical), 0, 2, 4, $\cdots$.

Fig. 2 $J^{(1)}$ and $J^{(2)}$ of the yrast SD ^{194}Hg(1). $J^{(1)}$ and $J^{(2)}$ are extracted directly from the experimental γ-ray energy using eqs. (1) and (2). $E_\gamma(I_0 + 2 \rightarrow I_0) = 254.3$ keV is the transition energies between the levels with spins $I_0 + 2$ and I_0, and I_0 is the spin of the lowest level observed in this SD band. The $J^{(1)}$-ξ and $J^{(2)}$-ξ plots for five spin assignments $I_0 = 8$, 9, 10, 11, and 12 are presented.

Fig. 3 $J^{(1)}$ and $J^{(2)}$ of the seven SD bands in the odd-Z nuclei: ^{191}Au(1), ^{191}Tl(1,2), ^{193}Tl(1,2), ^{195}Tl(1,2). $J^{(1)}$ and $J^{(2)}$ are extracted directly from the experimental γ-ray energy using eqs. (1) and (2). $E_\gamma(I_0 + 2 \rightarrow I_0)$ is the transition energy between the rotational levels with spins $I_0 + 2$ and I_0, and I_0 is the spin of the lowest level observed in this SD band. The $J^{(1)}$-ξ and $J^{(2)}$-ξ ($\xi = \sqrt{I(I+1)}$) plots for five assigned values of I_0 are presented. $J^{(1)}$ and $J^{(2)}$ are in units of $\hbar^2$MeV^{-1}.

Fig. 4 The same as Fig. 3, but for the four SD bands in the odd-N nuclei ^{189}Hg and ^{191}Hg: ^{189}Hg(1), ^{191}Hg(1), and signature partner ^{191}Hg(2,3).

Fig. 5 The same as Fig. 3, but for the five SD bands in the odd-N nucleus ^{193}Hg: ^{193}Hg(3), ^{193}Hg(2a), ^{193}Hg(2b), ^{193}Hg(1), and ^{193}Hg(4).

Fig. 6 The same as Fig. 3, but for the four SD bands in the even-even Hg nuclei:

^{190}Hg(1), ^{192}Hg(1), and signature partner ^{194}Hg(2,3).

Fig. 7 The same as Fig. 3, but for the four yrast SD bands in the even-even Pb nuclei: ^{192}Pb, ^{194}Pb, ^{196}Pb and ^{198}Pb.

Fig. 8 The same as Fig. 3, but for the three pairs of signature partner SD bands in the odd-odd nucleus ^{194}Tl: ^{194}Tl(1a), $E_\gamma(I_0+2 \rightarrow I_0) = 268.0$ keV, ^{194}Tl(2a), $E_\gamma(I_0+2 \rightarrow I_0) = 240.5$ keV, ^{194}Tl(3a), $E_\gamma(I_0+2 \rightarrow I_0) = 187.9$ keV, ^{194}Tl(1b), $E_\gamma(I_0+2 \rightarrow I_0) = 209.3$ keV, ^{194}Tl(2b), $E_\gamma(I_0+2 \rightarrow I_0) = 220.3$ keV, ^{194}Tl(3b), $E_\gamma(I_0+2 \rightarrow I_0) = 207.0$ keV.

Fig. 9 The same as Fig. 3, but for the three pairs of signature partner SD bands in the odd-odd nucleus ^{192}Tl: ^{192}Tl(1), $E_\gamma(I_0+2 \rightarrow I_0) = 357.8$ keV, ^{192}Tl(2), $E_\gamma(I_0+2 \rightarrow I_0) = 378.0$ keV, ^{192}Tl(3), $E_\gamma(I_0+2 \rightarrow I_0) = 375.7$ keV, ^{192}Tl(4), $E_\gamma(I_0+2 \rightarrow I_0) = 357.0$ keV, ^{192}Tl(5), $E_\gamma(I_0+2 \rightarrow I_0) = 381.2$ keV, ^{192}Tl(6), $E_\gamma(I_0+2 \rightarrow I_0) = 406.5$ keV.

Fig. 10 $\sqrt{J^{(1)3}/J^{(2)}}$-ξ plots of the three yrast SD bands: ^{189}Hg(1), ^{191}Hg(1), and ^{190}Hg(1) for five spin assignments. $J^{(1)}$ and $J^{(2)}$ are extracted directly from the experimental transition energy using eqs. (1) and (2) (see also Figs. 4 and 6).

Fig. 11 The odd-even differences in $J^{(1)}$ and $J^{(2)}$ at the spin values $I \sim 10$, 20, and 30. $J^{(1)}$ and $J^{(2)}$ are extracted from the experimental transition energy using eqs. (1) and (2) and the spin assignments presented in Table I. ∇ — SD band in ^{191}Au, — SD bands in ^{191,193,195}Tl, o — SD bands in ^{189,190,191,192,193,194}Hg, • — SD bands in ^{192,194,196}Pb.

Fig. 12 The I variation of $J^{(1)}$ and $J^{(2)}$ of the SD bands: ^{192}Hg(1), ^{194}Hg(1), ^{194}Hg(2), and ^{194}Hg(3). • and o denote the $J^{(1)}$ and $J^{(2)}$ extracted from the experimental transition energy using eqs. (1) and (2) and the spin assignments presented in Table I. The dotted line represents the calculated $J^{(1)}$ and $J^{(2)}$ using the analytic

expressions (32) and (33) (the values of the parameters a, b and c are given in Table II).

Fig. 13 Comparison between the moments of inertia of ^{194}Hg(2) and ^{192}Hg(1), and ^{194}Hg(3) and ^{192}Hg(1). o and ∇ are the extracted $J^{(1)}$ and $J^{(2)}$ of ^{192}Hg(1), respectively. • and are the extracted $J^{(1)}$ and $J^{(2)}$ of ^{194}Hg(2,3), respectively. The calculated $J^{(1)}$ and $J^{(2)}$ of ^{192}Hg(1) and ^{194}Hg(2,3) using the analytic expressions (32) and (33) are displayed by the dotted (^{192}Hg(1)) and solid (^{194}Hg(2,3)) lines (see also Fig. 12).

Fig. 14 The same as Fig. 13, but for the signature partner SD bands ^{191}Hg(2,3).

Fig. 15 The same as Fig. 13, but for the signature partner SD bands ^{193}Hg(2b) and ^{193}Hg(3).

Fig. 16 Comparison between the moments of inertia of the $[633]5/2^+$ band in ^{233}U and the ground state band of ^{236}U. The calculated $J^{(1)}$ and $J^{(2)}$ are practically the same as the extracted ones for the two bands in normally deformed nuclei.

Fig. 17 Comparison between the moments of inertia of the yrast SD bands: ^{194}Hg(1) and ^{192}Hg(1) (see also Fig. 13).

Fig. 18 The same as Fig. 17, but for the SD bands ^{194}Pb and ^{192}Hg(1).

Fig. 19 The same as Fig. 17, but for the SD bands ^{196}Pb and ^{198}Pb.

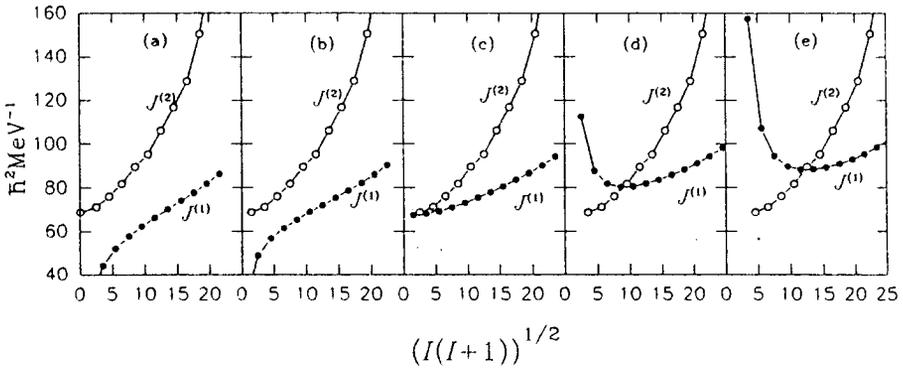

Fig. 1

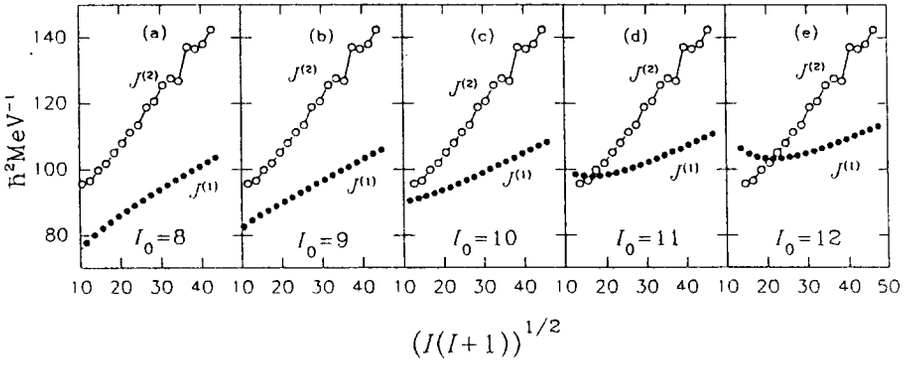

Fig. 2

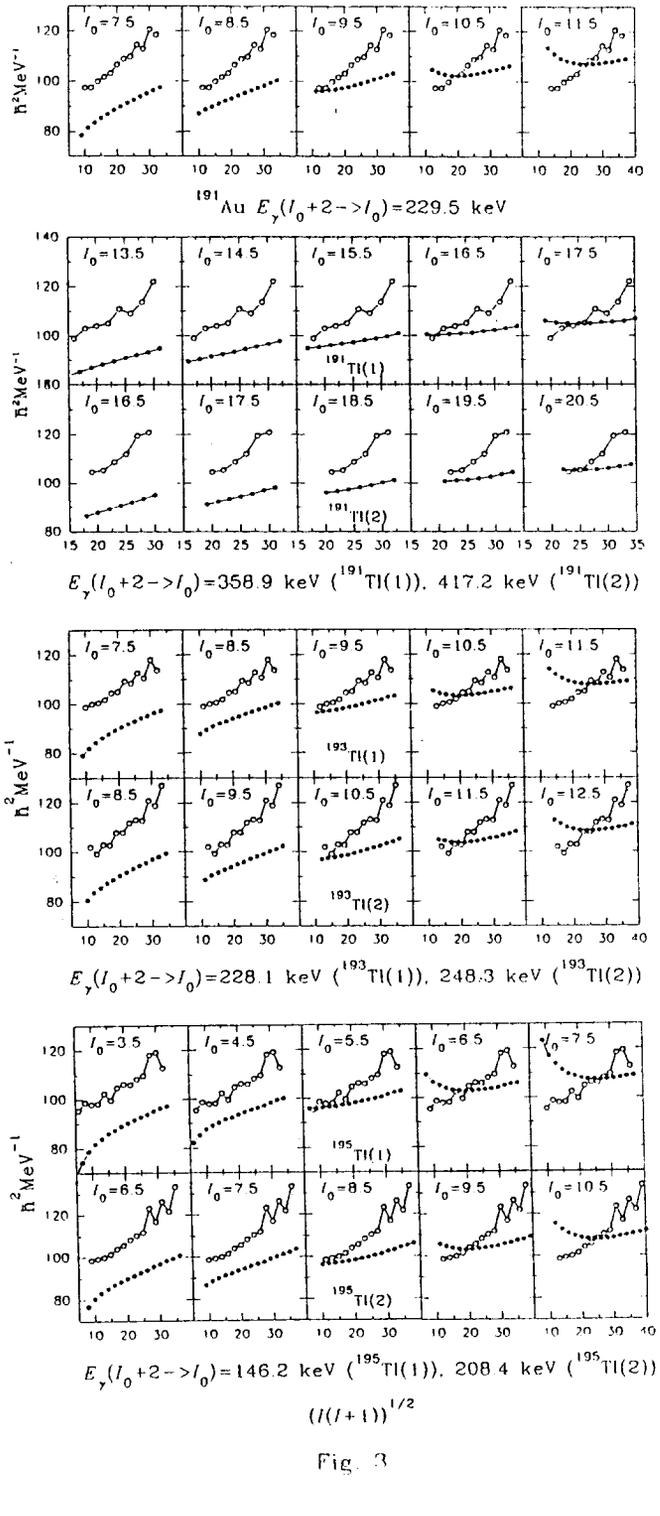

Fig. 3

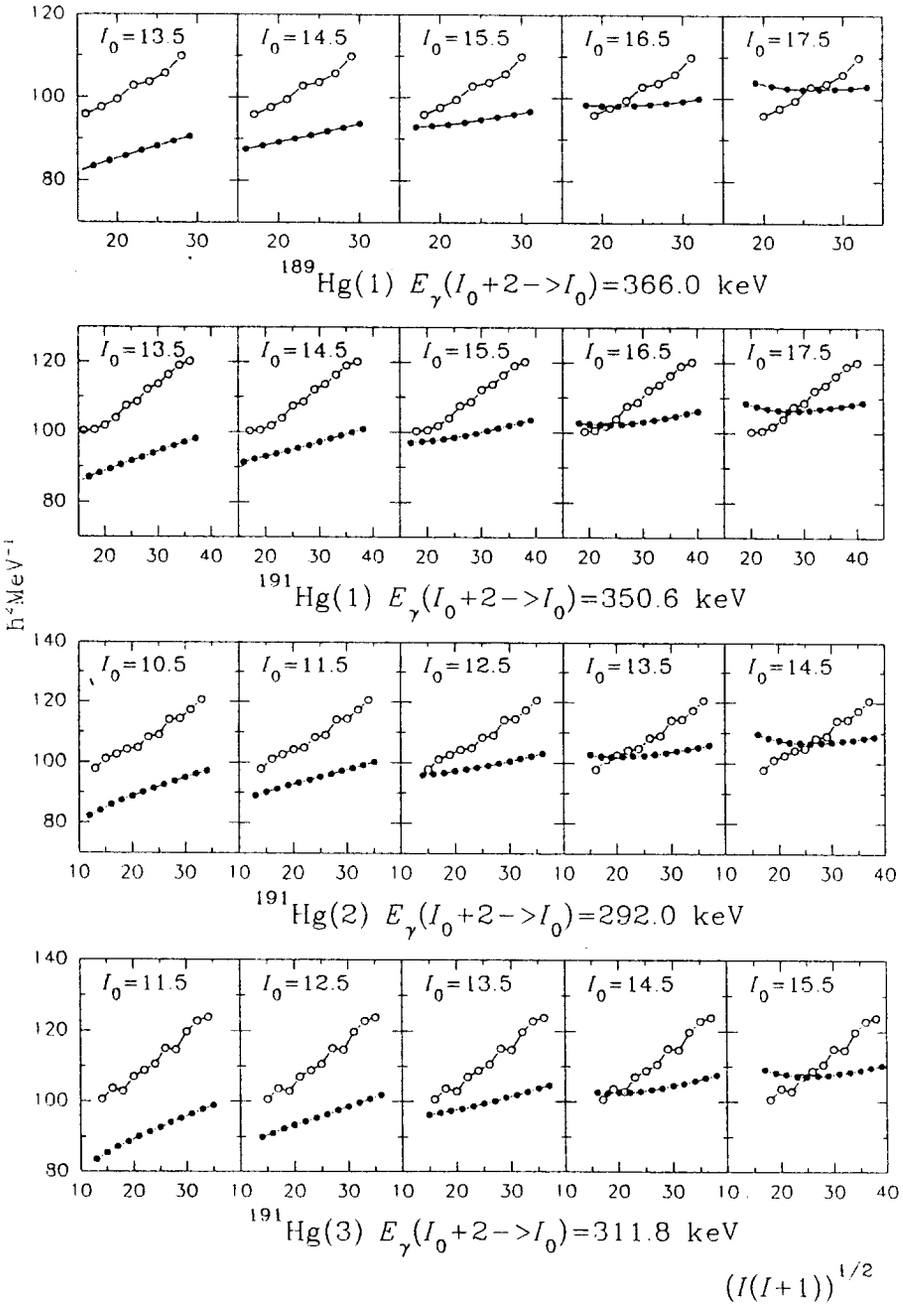
I_0=13.5
I_0=14.5
I_0=15.5
I_0=16.5
I_0=17.5
^{189}Hg(1) $E_\gamma(I_0+2->I_0)$=366.0 keV
I_0=13.5
I_0=14.5
I_0=15.5
I_0=16.5
I_0=17.5
^{191}Hg(1) $E_\gamma(I_0+2->I_0)$=350.6 keV
I_0=10.5
I_0=11.5
I_0=12.5
I_0=13.5
I_0=14.5
^{191}Hg(2) $E_\gamma(I_0+2->I_0)$=292.0 keV
I_0=11.5
I_0=12.5
I_0=13.5
I_0=14.5
I_0=15.5
^{191}Hg(3) $E_\gamma(I_0+2->I_0)$=311.8 keV
$\hbar^2$MeV^{-1}
$(I(I+1))^{1/2}$

Fig. 4

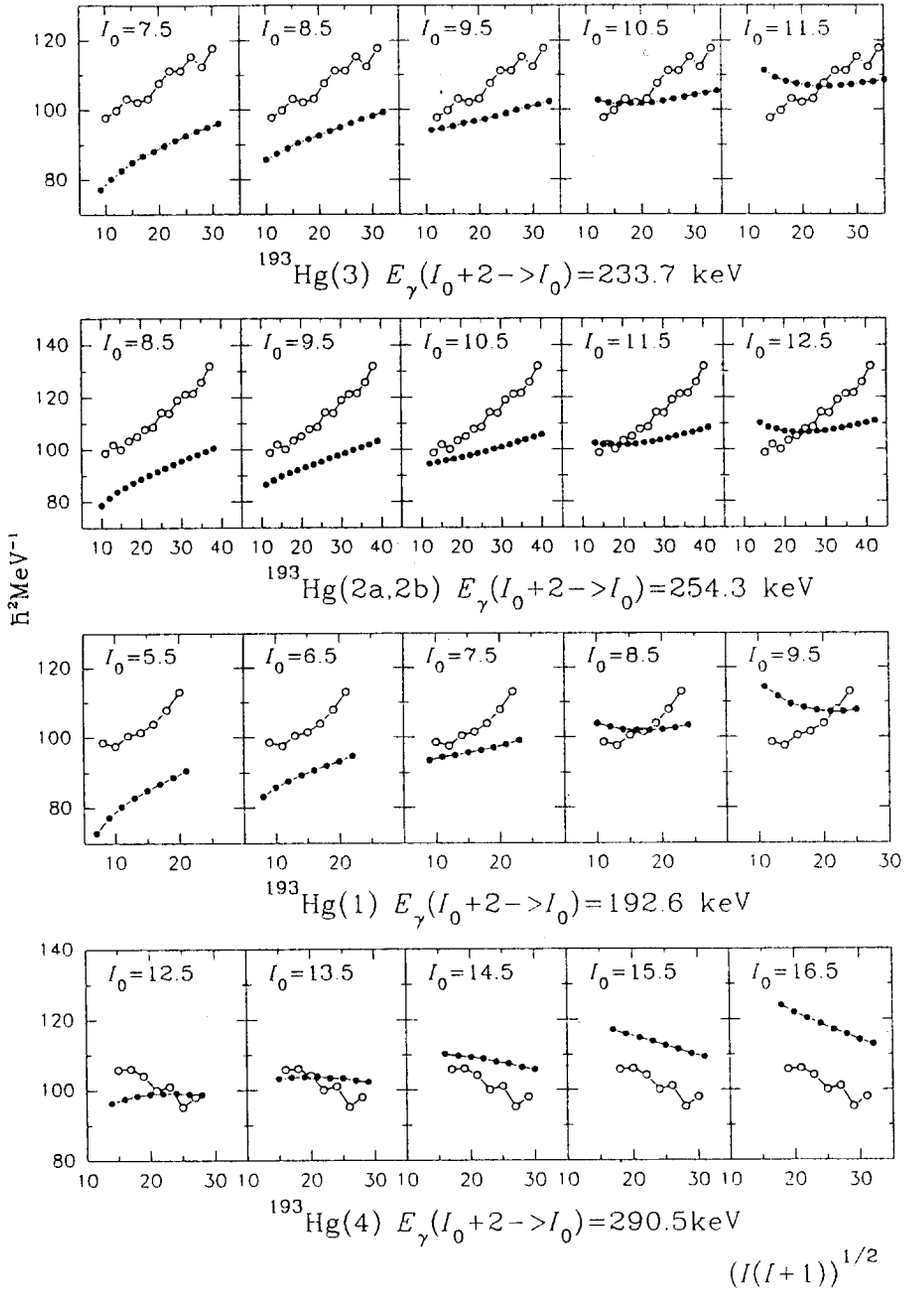
I_0=7.5
I_0=8.5
I_0=9.5
I_0=10.5
I_0=11.5
^{193}Hg(3) $E_\gamma(I_0+2->I_0)$=233.7 keV
I_0=8.5
I_0=9.5
I_0=10.5
I_0=11.5
I_0=12.5
^{193}Hg(2a,2b) $E_\gamma(I_0+2->I_0)$=254.3 keV
I_0=5.5
I_0=6.5
I_0=7.5
I_0=8.5
I_0=9.5
^{193}Hg(1) $E_\gamma(I_0+2->I_0)$=192.6 keV
I_0=12.5
I_0=13.5
I_0=14.5
I_0=15.5
I_0=16.5
^{193}Hg(4) $E_\gamma(I_0+2->I_0)$=290.5keV
$\hbar^2$MeV^{-1}
$(I(I+1))^{1/2}$

Fig. 5

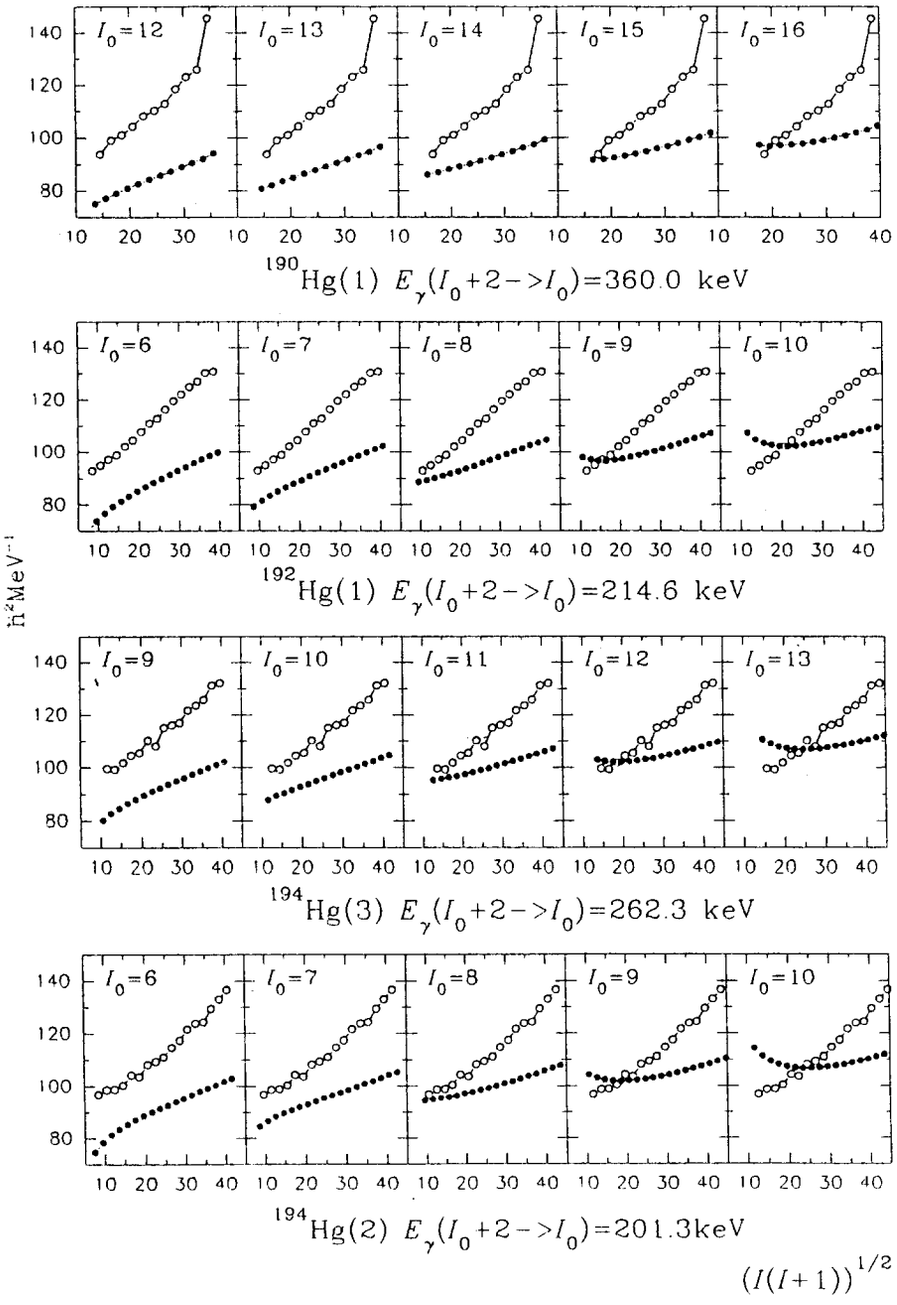
I_0=12
I_0=13
I_0=14
I_0=15
I_0=16
^{190}Hg(1) $E_\gamma(I_0+2->I_0)$=360.0 keV
I_0=6
I_0=7
I_0=8
I_0=9
I_0=10
^{192}Hg(1) $E_\gamma(I_0+2->I_0)$=214.6 keV
I_0=9
I_0=10
I_0=11
I_0=12
I_0=13
^{194}Hg(3) $E_\gamma(I_0+2->I_0)$=262.3 keV
I_0=6
I_0=7
I_0=8
I_0=9
I_0=10
^{194}Hg(2) $E_\gamma(I_0+2->I_0)$=201.3keV
$\hbar^2$MeV^{-1}
$(I(I+1))^{1/2}$

Fig. 6

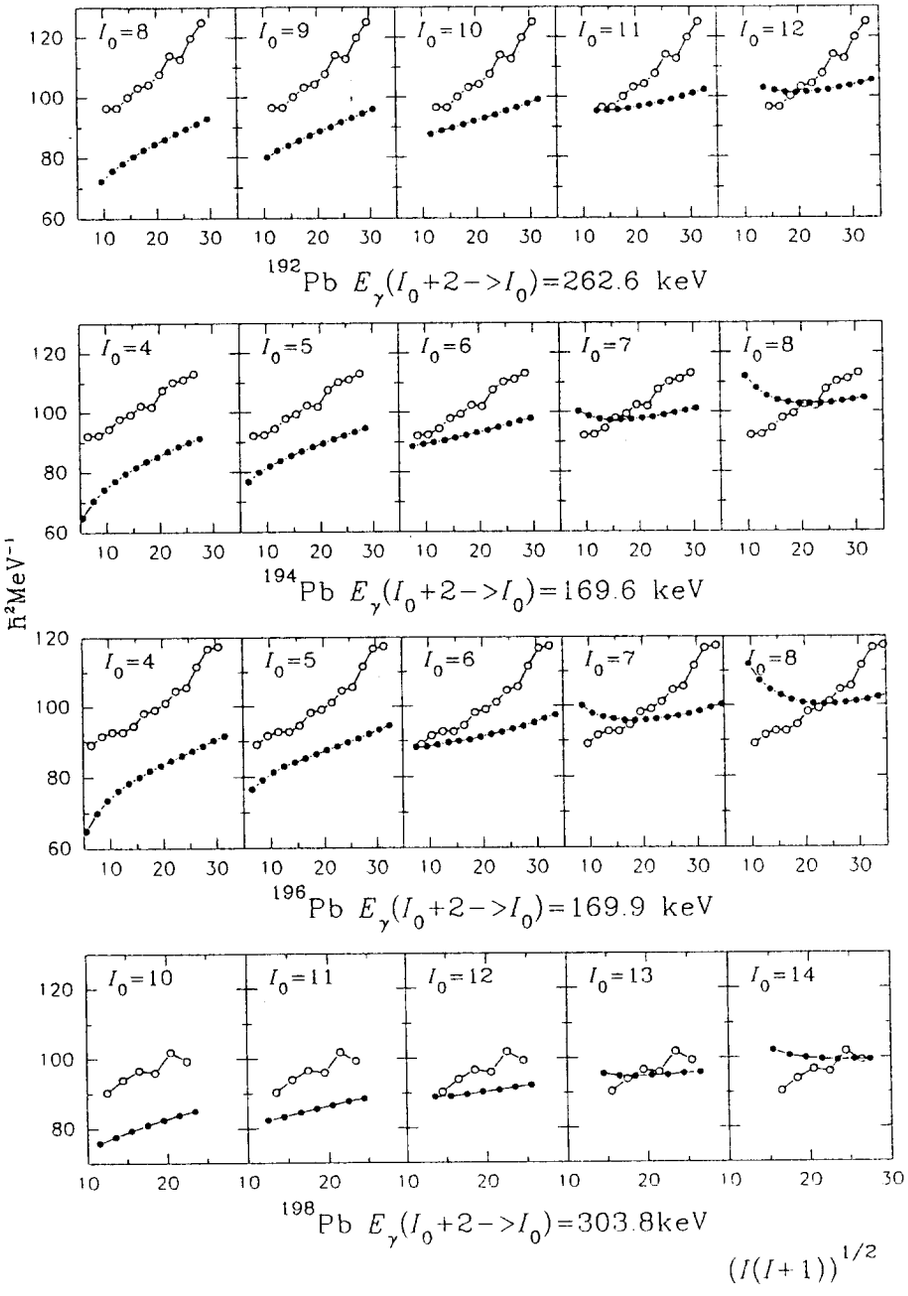
I_0=8
I_0=9
I_0=10
I_0=11
I_0=12
^{192}Pb $E_\gamma(I_0+2->I_0)$=262.6 keV
I_0=4
I_0=5
I_0=6
I_0=7
I_0=8
^{194}Pb $E_\gamma(I_0+2->I_0)$=169.6 keV
I_0=4
I_0=5
I_0=6
I_0=7
I_0=8
^{196}Pb $E_\gamma(I_0+2->I_0)$=169.9 keV
I_0=10
I_0=11
I_0=12
I_0=13
I_0=14
^{198}Pb $E_\gamma(I_0+2->I_0)$=303.8keV
$\hbar^2$MeV^{-1}
$(I(I+1))^{1/2}$

Fig. 7

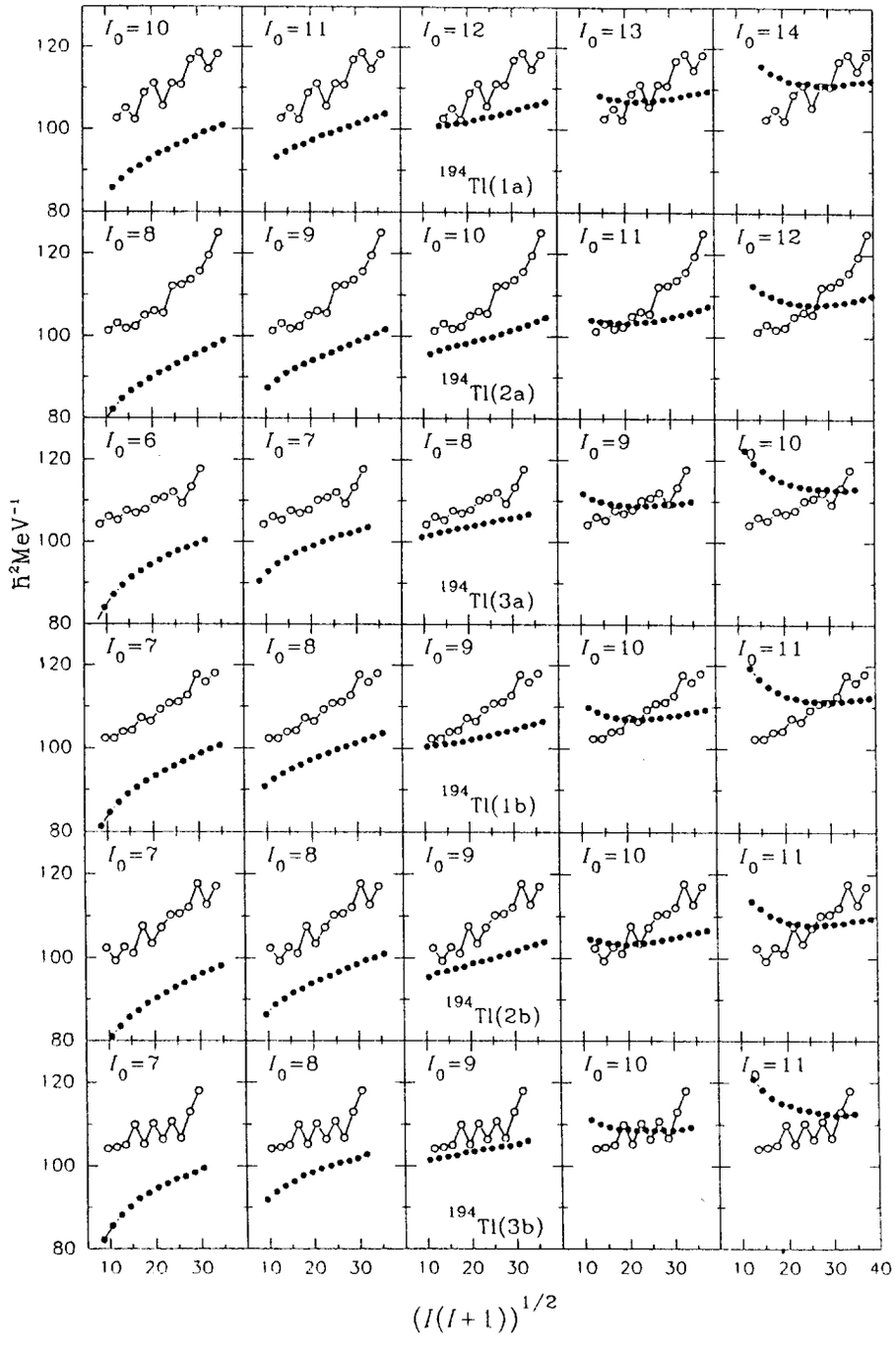
$I_0=10$
$I_0=11$
$I_0=12$
$I_0=13$
$I_0=14$
^{194}Tl(1a)
$I_0=8$
$I_0=9$
$I_0=10$
$I_0=11$
$I_0=12$
^{194}Tl(2a)
$I_0=6$
$I_0=7$
$I_0=8$
$I_0=9$
$I_0=10$
^{194}Tl(3a)
$I_0=7$
$I_0=8$
$I_0=9$
$I_0=10$
$I_0=11$
^{194}Tl(1b)
$I_0=7$
$I_0=8$
$I_0=9$
$I_0=10$
$I_0=11$
^{194}Tl(2b)
$I_0=7$
$I_0=8$
$I_0=9$
$I_0=10$
$I_0=11$
^{194}Tl(3b)
$\hbar^2$MeV^{-1}
$(I(I+1))^{1/2}$

Fig 8

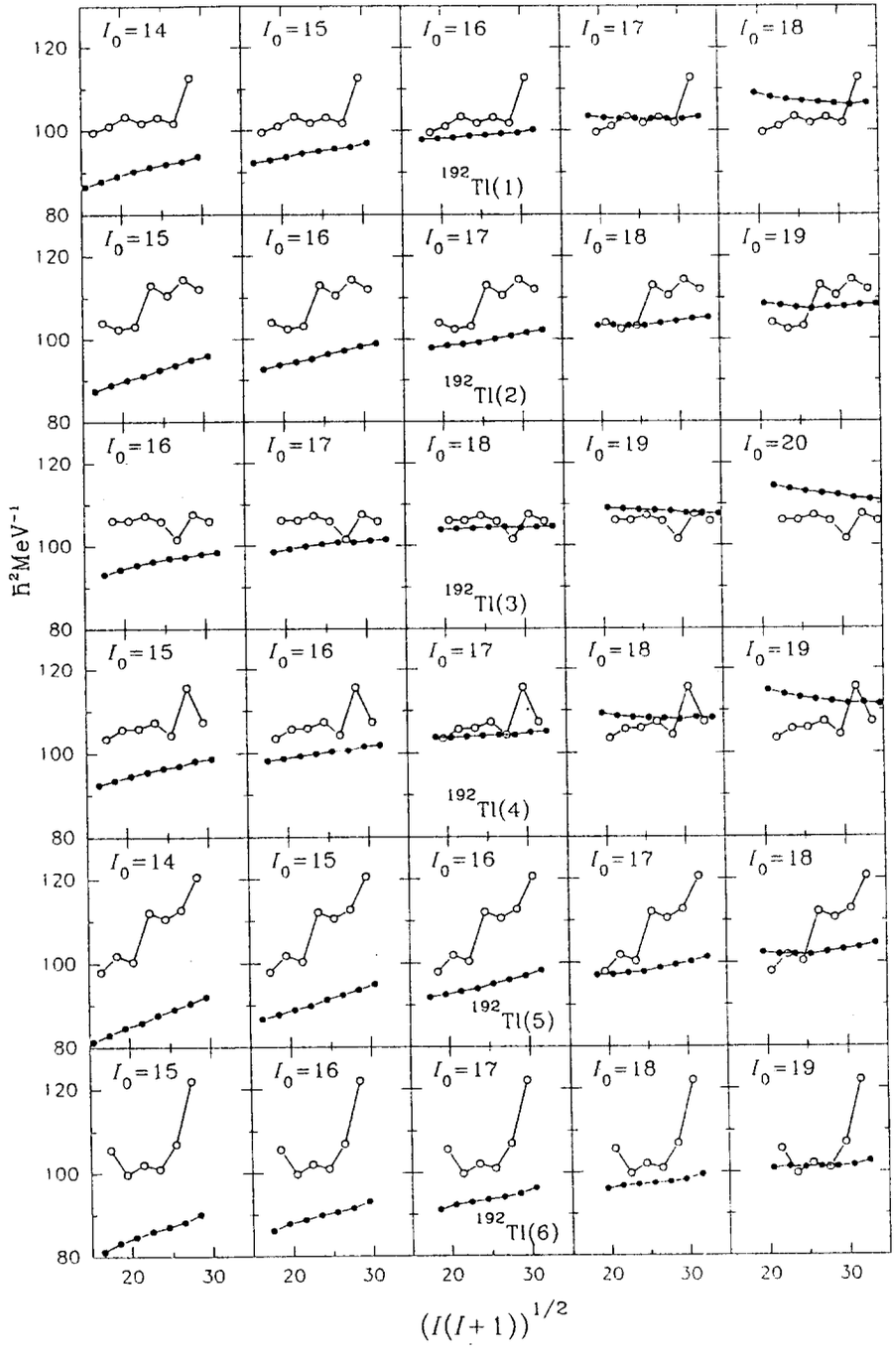
$I_0=14$
$I_0=15$
$I_0=16$
$I_0=17$
$I_0=18$
^{192}Tl(1)
$I_0=15$
$I_0=16$
$I_0=17$
$I_0=18$
$I_0=19$
^{192}Tl(2)
$I_0=16$
$I_0=17$
$I_0=18$
$I_0=19$
$I_0=20$
^{192}Tl(3)
$I_0=15$
$I_0=16$
$I_0=17$
$I_0=18$
$I_0=19$
^{192}Tl(4)
$I_0=14$
$I_0=15$
$I_0=16$
$I_0=17$
$I_0=18$
^{192}Tl(5)
$I_0=15$
$I_0=16$
$I_0=17$
$I_0=18$
$I_0=19$
^{192}Tl(6)
$\hbar^2$MeV^{-1}
$(I(I+1))^{1/2}$

Fig 9

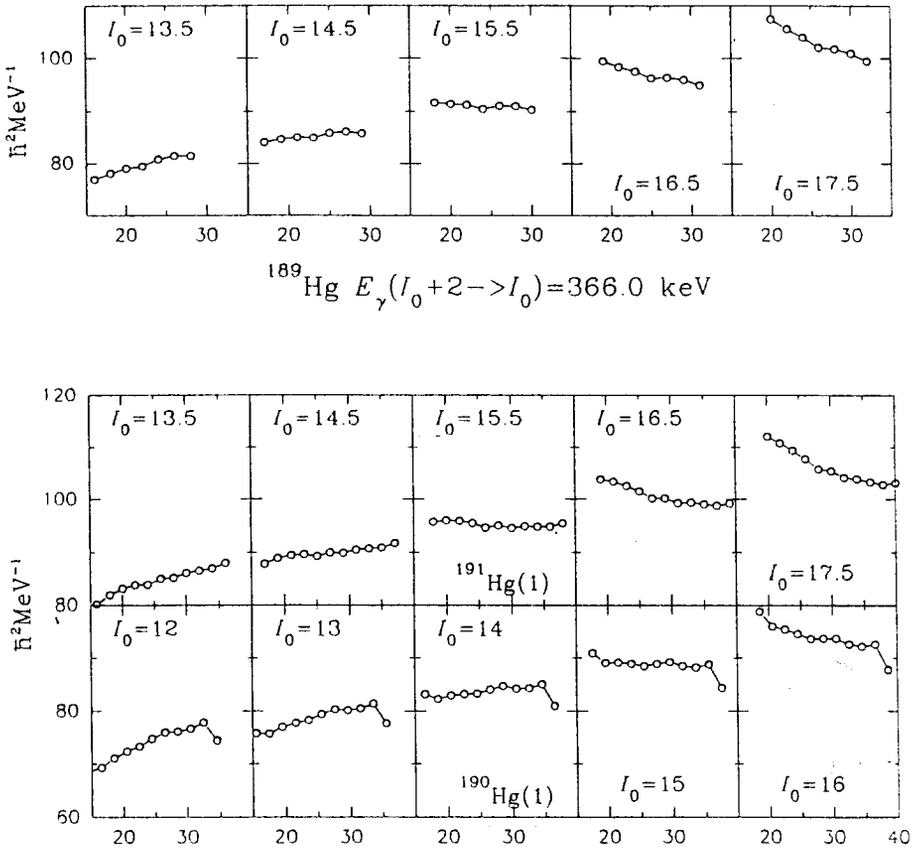
I_0=13.5
I_0=14.5
I_0=15.5
I_0=16.5
I_0=17.5
$\hbar^2$MeV^{-1}
^{189}Hg $E_\gamma(I_0+2->I_0)$=366.0 keV
I_0=12
I_0=13
I_0=14
I_0=15
I_0=16
^{191}Hg(1)
^{190}Hg(1)
$E_\gamma(I_0+2->I_0)$=350.6 keV (^{191}Hg(1)), 360.0 keV (^{190}Hg(1))
$(I(I+1))^{1/2}$

Fig. 10

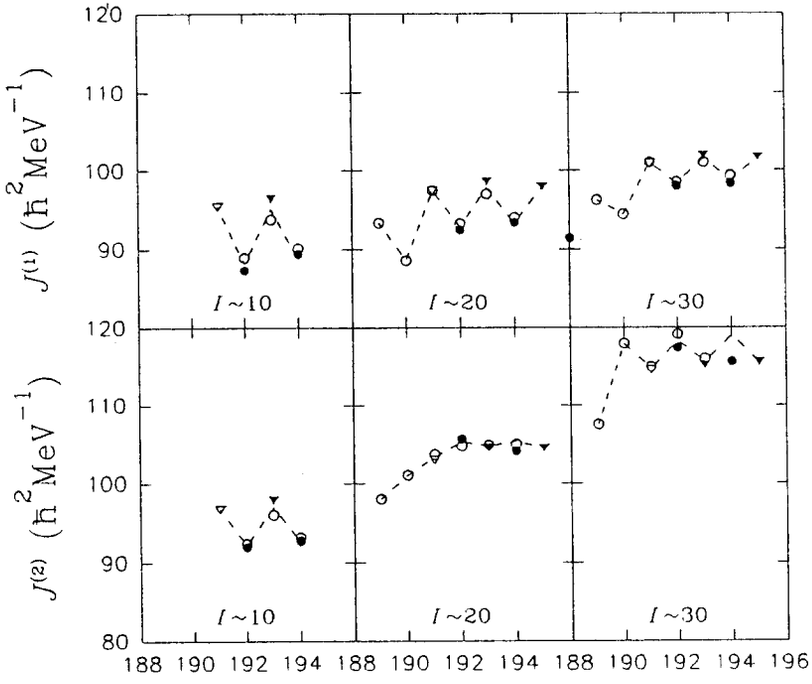
$J^{(1)}$ ($\hbar^2$MeV^{-1})
$J^{(2)}$ ($\hbar^2$MeV^{-1})
I~10
I~20
I~30
A

Fig. 11

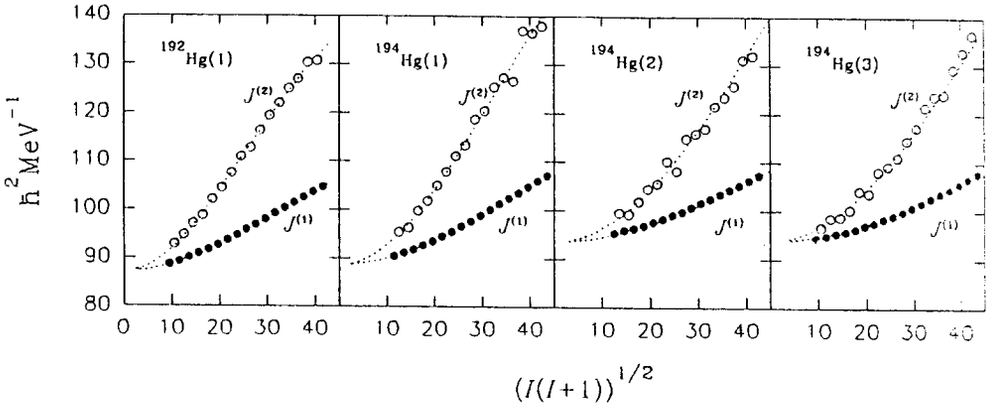

Fig. 12

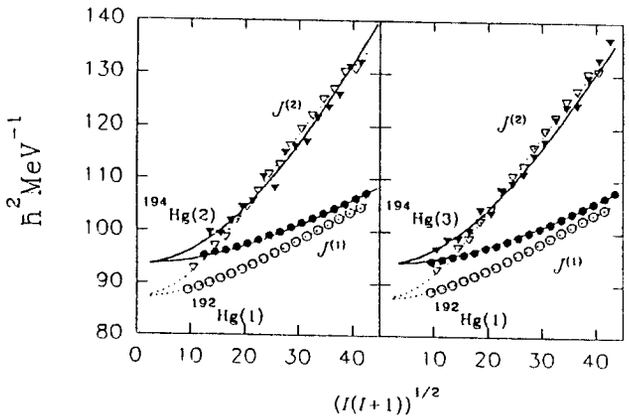

Fig. 13

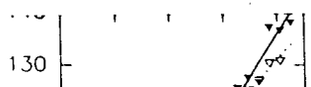

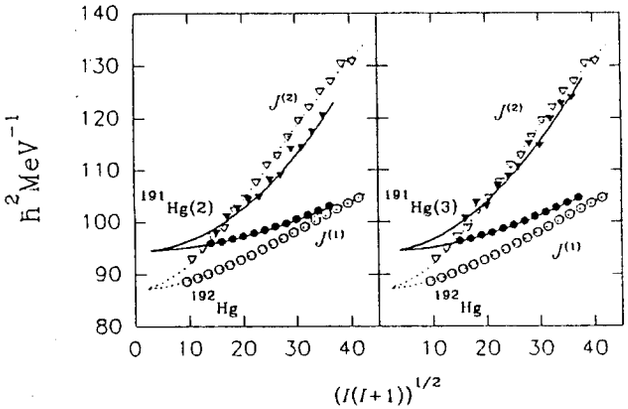

Fig. 14

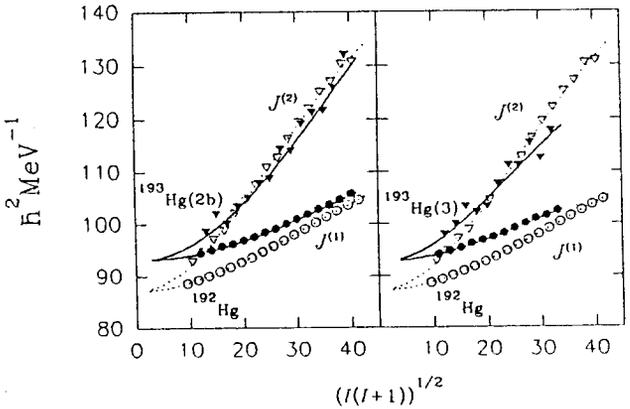

Fig. 15

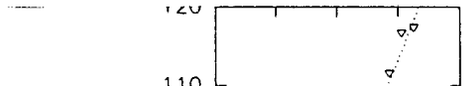

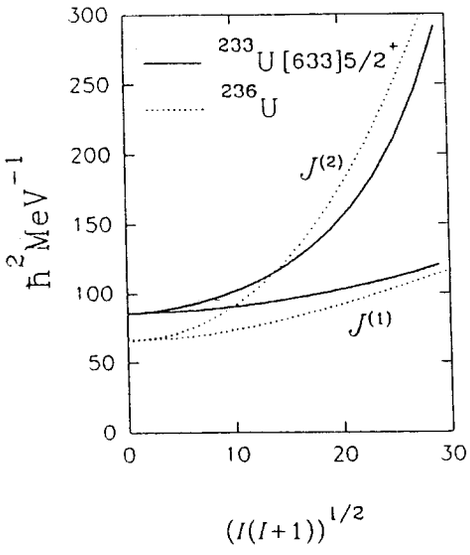

Fig. 16

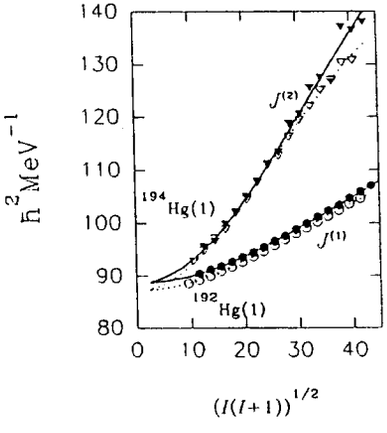

Fig. 17

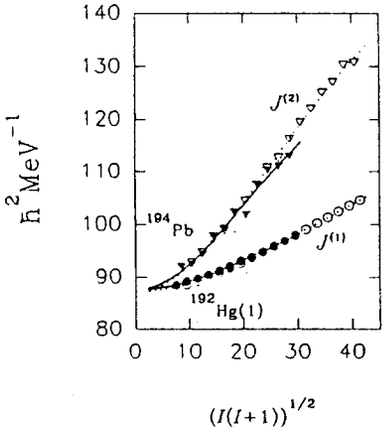

Fig. 18

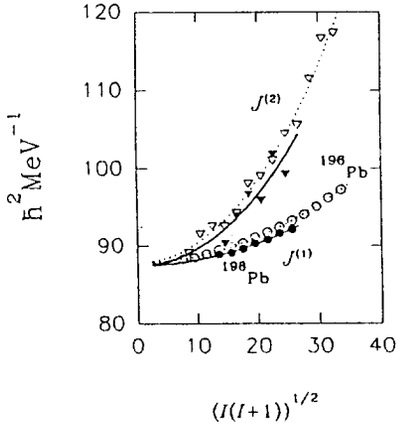

Fig. 19